Microgrid Power Flow Control with Integrated Battery Management Functions

Qian Long*, Hui Yu*, Fuhong Xie*, Wente Zeng†, Srdjan Lukic*, Ning Lu* and David Lubkeman*
*Department of Electrical and Computer Engineering, North Carolina State University, Raleigh, NC
†Total New Energies Ventures USA, San Francisco, CA

***Abstract*—This paper presents a microgrid power flow control for islanded microgrids consisting of photovoltaic (PV) system, battery energy storage system (BESS) and diesel generator. The proposed control ensures automatic coordination among the microgrid units. To achieve the coordination, the local control of PV system and BESS are configured to regulate power flow without relying on communications. The generator is controlled as the back-up source and its connection depends on battery state of charge (SOC). A state machine with hysteresis settings is used to trigger smooth transition among operation modes. Not only does the proposed controller consider battery SOC and power limits, but also integrates three-stage charging control as battery charging mechanism, which is not considered in the existing literature. The proposed control is validated for an islanded hybrid microgrid using an OPAL-RT real-time simulator.**

***Index Terms*—Power flow control, three-stage charging control, islanded hybrid microgrids**

I. Introduction

Islanded hybrid microgrids, consisting of photovoltaic (PV) systems, battery energy storage systems (BESS) and diesel generators, present a clean and economical approach to power rural areas where the utility service is inaccessible or has poor quality [1]. While the integration of PV system and BESS provides flexibility of supplying energy, the diesel generator can be used as the back-up source when an islanded microgrid faces energy deficit problems. Power management, as a critical application to islanded microgrid operation, coordinates output power of these microgrid units while maintaining system frequency and voltage. However, how to properly integrate the constraints of BESS into power flow control still needs to be considered.

Microgrid power flow control in islanded microgrids has been widely studied using centralized architecture [2]–[4]. Under this architecture, the communication links between microgrid controller and each microgrid component are required to coordinate the operation of microgrid units. In [2], a centralized power management control has been implemented into an embedded microcontroller. The state of charge (SOC) management is achieved by dispatching the fuel-cell system. However, the BESS power limiting function is not explored because it is assumed that the PV system has lower rated power than the battery maximum charging power. Another centralized power management system is proposed in [3] to coordinate hybrid PV-battery unit with the generator. While the SOC management is integrated into the BESS local control, the power limiting functions for the BESS and the generator are not carefully considered in the study. An adaptive coordination scheme is described in [4] to achieve close frequency regulation as well as SOC and power limiting functions. To manage high SOC scenarios, battery charging power is set directly to zero. However, this charging control is not realistic since the battery management system (BMS) in reality might still allow the battery to be charged.

The other approach of solving coordination issues is through decentralized power management control. This approach requires no information exchange between units or between a unit and a centralized control entity, but takes advantage of the fact that each microgrid unit shares a universal frequency across the system. A Fuzzy-Logic controller based on frequency-signal techniques is developed in [5] to manage power flow of an islanded microgrid with a PV system, a BESS and a microturbine unit while considering battery maximum power limit and SOC limit. The authors in [6] introduced a decentralized method to achieve power flow control in an islanded microgrid consisting of multiple PV units, battery units and PV/battery hybrid units. Discrete control modes are defined, and adaptive droop control is employed in each control mode to respect the SOC and power limits of BESS units. Multi-segment adaptive droop control is proposed in [7], [8] as a fully decentralized control strategy to fit into islanded microgrids with a general structure (i.e. multiple PV units, battery units, hybrid PV/battery units and conventional droop-controlled generators). The strategy also ensures that the operation constraints of each BESS are complied with. Although all these strategies mentioned above consider battery SOC and power limits in their designs, a three-stage charging control, which is a realistic charging mechanism of BMS, is not studied. The lack of this mechanism might still lead to inappropriate charging, poor battery voltage regulation and reduced life-time of the battery system.

The paper proposes a novel microgrid power flow control that integrates realistic battery management functions with the proper coordination of multiple operation modes for islanded microgrids. Section II describes the assumed operating modes of the microgrid. Section III provides the design details of the proposed microgrid power flow control, especially regarding integration of three-stage charging control while considering the coordination with other operation modes. Section IV presents real-time simulation results for an islanded microgrid with the proposed controller. Section V concludes the paper.

II. Microgrid System Overview

The system schematic of the islanded hybrid microgrid is shown in Fig. 1, where the component sizes are given to represent the studied microgrid in Section IV. PV arrays are

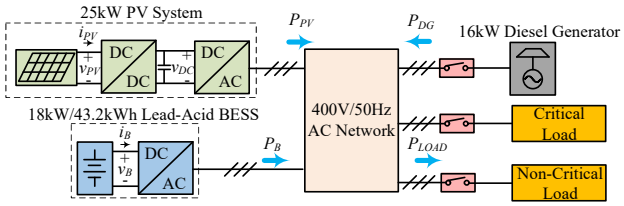

Fig. 1: Microgrid system diagram

interfaced with the microgrid AC bus by a two-stage DC/AC inverter. A battery unit is connected to the AC bus using a single-stage DC/AC inverter. The connection to the AC bus is controlled by a relay for either the generator unit or the load.

The assumed operation of the microgrid is described as follows:

1) The operation mode of the PV system is only decided by the frequency. Overfrequency events activate the frequency-watt (freq-watt) curtailment. Otherwise, the PV system operates under MPPT control. The first stage of the PV system, the DC-DC converter, is controlled by either the MPPT controller or the freq-watt curtailment controller. The second stage of the PV system, the three-phase DC-AC inverter, is modeled as a grid-feeding unit regulating the DC link capacitor voltage and injecting power into the system.
2) The BESS is the master unit providing the frequency and voltage reference of the microgrid AC bus when the generator is offline. The droop control is implemented in the battery inverter to achieve seamless transition between non-generator operation and generator-connected operation. The secondary control of the battery inverter is developed for multiple purposes. In general, the secondary control is able to bring the frequency and voltage back to nominal value. However, the secondary control also enables other microgrid operation modes when needed, such as generator synchronization and three-stage charging control. Once the generator is online and connected, the BESS switches to power dispatch mode where it follows the real and reactive power setpoints.
3) The generator, as a back-up source, only starts at a low SOC level. The generator synchronization is achieved by the battery inverter. The relay closes automatically when there is sufficiently small voltage angle and magnitude difference on both sides of the generator breaker. Note that the generator in this study is an isochronous generator, consisting of an isochronous speed control and an excitation system. The generator relay is set to trip the generator whenever its output current exceeds the maximum allowable current or goes into a reverse direction.
4) The load is fully supplied in most situations. The non-critical load is only curtailed in generator-connected operation when there is a extremely low SOC level.

Table I summarizes all the microgrid operation modes. In Mode 1, the generator is turned off. The full load is supplied since the battery SOC is at a relatively high level. The BESS regulates voltage and frequency and compensates any power difference between PV generation and load consumption. However, the output power of the BESS should always conform to its rated capacity and also, more importantly, the maximum allowable charging power. Under constant power charging, the maximum allowable charging power is equal to the rated capacity of the battery inverter, while under constant voltage charging, the maximum allowable charging power is a variable limit. If the BESS output power violates the maximum allowable charging power, the battery inverter increases system frequency to curtail PV power.

TABLE I: Microgrid operation modes

Mode	BESS	PV System	Generator	Loads
Mode 1	V/f regulation	decided by f	offline	full
Mode 2	P dispatch	MPPT	V/f regulation	full
Mode 3	P dispatch	MPPT	V/f regulation	critical
Mode 4	offline	offline	offline	offline

In Mode 2, the battery SOC is at a relatively low SOC level. The generator becomes the master unit to regulate voltage and frequency and to compensate any power difference among the PV system, the BESS and the load. Since the generator provides fixed system frequency in this mode, the PV system only operates under MPPT control. The BESS in Mode 2 acts as a grid-feeding unit and its power dispatch strategy will be discussed in the next section. The only difference between Mode 3 and Mode 2 is that all the non-critical loads are shed in Mode 3. Mode 4 represents the mode where all the units are shut down and disconnected.

III. Microgrid Power Flow Control with Integrated BMS

The challenge of integrating three-phase charging control in islanded microgrids is to have the grid-forming battery inverter regulate output power while maintaining voltage and frequency regulation. Also, with irradiance and load variations, the three-stage charging control should be able to adapt to different operating conditions. To achieve that, both the PV control and the BESS control are configured in a coordinated way such that BESS is able to indirectly control its output power by controlling system frequency. This section discusses the details of this control design and implementation.

A. Local PV Control

A two-stage three-phase PV inverter is utilized, as shown in Fig. 1, . The DC-DC boost converter is controlled by either the MPPT controller or the freq-watt curtailment control. The inverter control is implemented using the dual-loop controller for DC capacitor voltage regulation.

The control diagram for the first stage of the PV inverter is shown in Fig. 2. It consists of the MPPT controller, which is implemented using a data-driven MPP estimation algorithm, and the freq-watt curtailment control. The final PV real power setpoint is jointly determined by both the MPPT control and the frequency curtailment control. The PI control regulates the

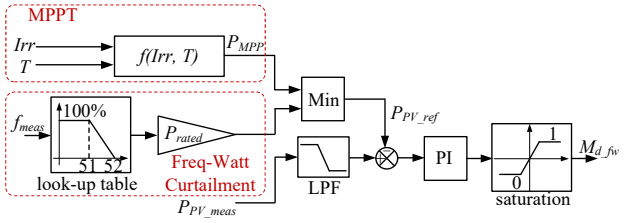

Fig. 2: Control diagram for the PV DC-DC converter

DC output power from the PV arrays based on the final real power setpoint.

The look-up table, shown in Fig. 2, determines a piece-wise linear relationship between frequency and real power curtailment during an over-frequency period. The freq-watt curtailment only takes effect when the frequency goes above 51Hz. Between 51Hz and 52Hz, there is a proportional decrease in the PV output power as the frequency increases. Above 52Hz, the PV power is fully curtailed. However, the freq-watt curtailment is still subject to MPPT control. During the PV real power curtailment, it is still possible that the power setpoint is determined from the MPPT control rather than from the freq-watt curtailment because the PV output power can be no greater than the maximum available power. The advantage of this control design is that it avoids the two PV control modes from switching back and forth and enables automatic adaptation to irradiance variations.

B. Local BESS Control

As discussed in Section II, two different control modes exist in the BESS depending on the status of the diesel generator. When the generator is offline, the BESS adopts a frequency-based power management method in coordination with the PV system; when the generator is online, the BESS directly follows the power setpoints. A complete control structure that achieves smooth transition between different modes is proposed here.

1) Control Strategy in Mode 1: Fig. 3 illustrates the frequency generation control that takes the battery three-stage charging function into account. Firstly, the constant power mode is activated when battery SOC is considerably low. The BESS is charged by available power in the system, which is no more than the battery inverter rated power P_{rated}. A PI controller is implemented here to achieve the power limiting control. The output of the PI controller is the frequency deviation Δf_1, which will be added to the nominal frequency f_{nom} later to generate the required frequency reference f_{ref}. Under constant power mode, as the battery SOC increases, the battery voltage V_{batt} also increases and the battery inverter finally goes to constant voltage mode. In this mode, battery voltage will be clamped to a reference value V_{batt_ref} by using another PI controller to generate the corresponding frequency deviation Δf_2. This frequency deviation Δf_2 will be compared with Δf_1. When Δf_2 is larger than Δf_1, the charging control will transition from constant power mode to constant voltage mode. Lastly, when battery SOC further increases and becomes higher than a predefined threshold, the

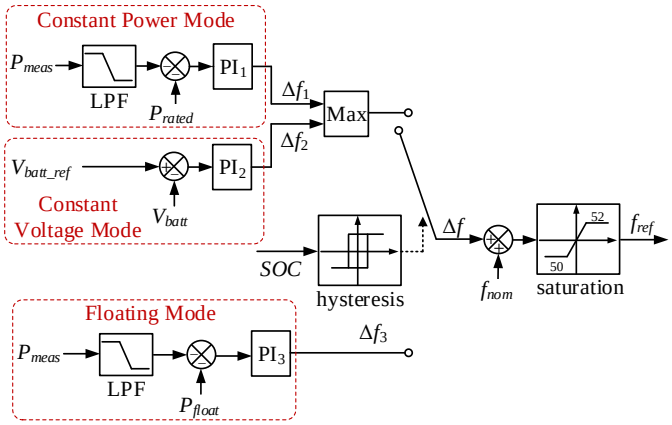

Fig. 3: Battery inverter frequency reference generation control

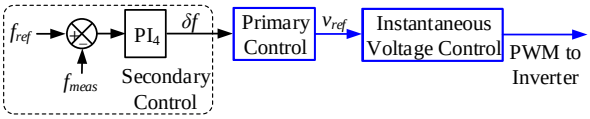

Fig. 4: Hierarchical frequency control structure

charging control enters floating mode with minimal charging power P_{float}. A third PI controller is implemented here to regulate the charging power to P_{float}. A switch triggered by SOC is implemented for selection between the former two modes and the floating mode. A hysteresis block is adopted to avoid frequent mode switch. A saturation block is implemented to limit the system frequency reference within the range between 50Hz to 52Hz to be consistent with PV freq-watt curtailment.

The frequency reference f_{ref} generated in Fig. 3 will be sent to a hierarchical frequency control structure, as shown in Fig. 4. The control objective is to make the measured system frequency f_{meas} precisely follow the frequency reference. A PI controller is implemented as the secondary controller, the output of which will be sent to the primary control to generate the instantaneous voltage reference. The voltage control regulates the inverter output voltage to desired voltage magnitude and frequency. Details of primary control and voltage tracking control are omitted here, but can be found in [9], [10].

2) Control Strategy in Mode 2 and 3: Under this condition, the isochronous generator provides voltage and frequency references for the rest of the system, both of which are designed to be at their nominal values. With voltage and frequency references, the BESS can easily track the power setpoints using primary control [10]. Similar to the case without the generator, a three-stage charging control structure is proposed. With low SOC, the charging control is in constant power mode and the power reference is selected from the smaller value between P_{rated} and $90\%P_{gen\_rated} + P_{pv} - P_{load}$. As both the SOC and battery terminal voltage increase, the constant voltage mode might be triggered, for which case a PI controller is implemented to generate a power reference and clamp the voltage to its reference V_{batt_ref}. When the battery is almost fully charged, the charging control enters floating mode. A hysteresis-based switch triggered by SOC is implemented for

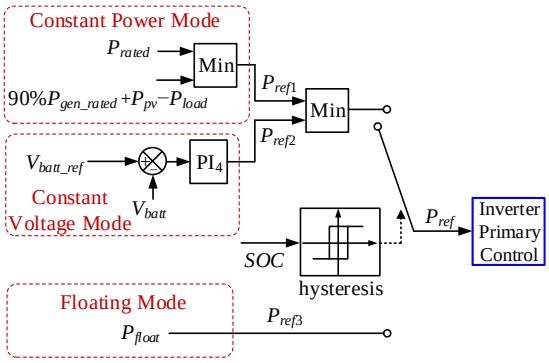

Fig. 5: Three-stage charging with diesel generator

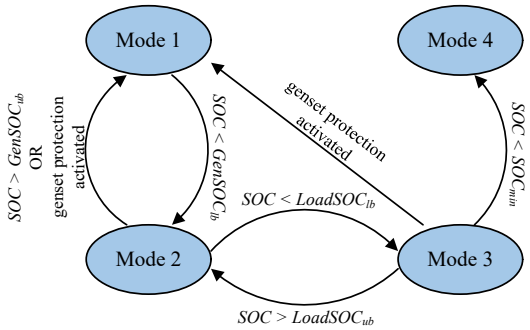

Fig. 6: Microgrid control state machine

smooth transition between different modes.

C. Smooth Mode Transitions

The state machine for the microgrid power flow controller is depicted in Fig. 6 and all the operation modes correspond to Table I. Battery SOC is the main trigger for state transitions. To ensure smooth state transition, SOC settings with hysteresis are applied to transitions between Mode 1 and Mode 2. In order to bring the generator online, the battery SOC must be lower than the lower bound $GenSOC_{lb}$. However, when the battery SOC is above this threshold, the generator would not be disconnected until the SOC exceeds the upper bound $GenSOC_{ub}$. The similar hysteresis settings $LoadSOC_{lb}$ and $LoadSOC_{ub}$ are applied to transitions between Mode 2 and Mode 3. Note that in moving from Mode 1 to Mode 2, there are a series of actions in terms of the battery inverter synchronizing with the generator. The resynchronization strategy in [9] is employed in this paper.

Besides triggered by SOC, Mode 1 can be transitioned to from Mode 2 or Mode 3 whenever the generator is tripped by the overcurrent/undercurrent protection. The overcurrent protection guarantees the generator output current will not exceed its maximum output current while the undercurrent protection avoids the output current in the reverse direction. Mode 4, in which the whole microgrid is shut down, can only be entered from Mode 3 when battery SOC is below SOC_{min}.

IV. Real-Time Simulation Results

The proposed method has been evaluated using an OPAL-RT real-time simulator with the schematic as shown in Fig. 1. Two case studies are performed to evaluate the performance of the proposed microgrid power flow control under different operating conditions. In the first case study, the three-stage charging mechanism is studied with PV and load variations. The second case study evaluates the performance that includes the transition among multiple operating modes.

A. Smooth Charging Control with Irradiance and Load Variations

Fig. 7(a) shows the output power of the PV system and the BESS as well as load consumption. Initially, the output power of the PV system under MPPT mode is equal to 15kW and load consumption is equal to 2kW. As the grid-forming device, the battery unit is charged by 13kW. At t = 0.28h (1000s), the irradiance is increased from 600W/m^2 to 1000W/m^2. The battery charging power is temporarily increased to 22.8kW, followed by a decrease to 18kW due to the effect of the proposed control. As is shown in Fig. 7(b), the frequency of the islanded microgrid settles at 51.3Hz. After t = 0.69h (2500s), there are a sequence of load switching actions. For a load decrease, the BESS increases the frequency to curtail PV generation. For a load increase, the BESS first decreases the frequency to release PV generation. Once PV generation is fully released, the battery inverter starts to decrease its charging power to compensate for the increase of load consumption. At t = 1.03h (3700s) when load consumption keeps increasing, the battery inverter decreases the frequency back to 50Hz and changes from being charged to being discharged. The subsequent load decrease causes the BESS to start charging. After the charging power hits the battery inverter rated power, the frequency is increased again to curtail PV generation.

Fig. 7(a) shows that at t = 1.69h (6100s), the charging control switches from constant power charging to constant voltage charging. During the constant voltage charging, the charging power decreases exponentially. Note that small load variations have no impact on battery charging power during constant voltage charging as long as there are still available reserves from the PV system. However, a large load step during constant voltage charging can possibly change the BESS from being charged to being discharged. At t = 2.69h (9700s), the battery goes into float mode where there is only a minimal charging power flowing into the battery unit. Fig. 7(c) illustrates battery terminal voltage during the process. Although there are transients initiated by load switching actions, no significant overvoltage is observed.

B. Transition of Multiple Operation Modes

Fig. 8 shows component power levels for different mode transitions of the islanded microgrid. In the beginning of the simulation, since PV generation is high, the constant power charging is triggered with the charging power limit imposed. At t = 0.09h (310s), as the load increases, PV generation is released and the BESS changes from being charged to being discharged, similar to the first case. To force the microgrid to transition from Mode 1 into Mode 2, the load is kept at maximum level to keep the discharging of the BESS. At t = 0.96h (3400s) when battery SOC hits the lower bound

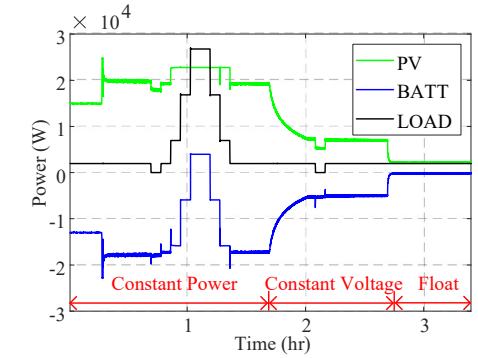

(a)

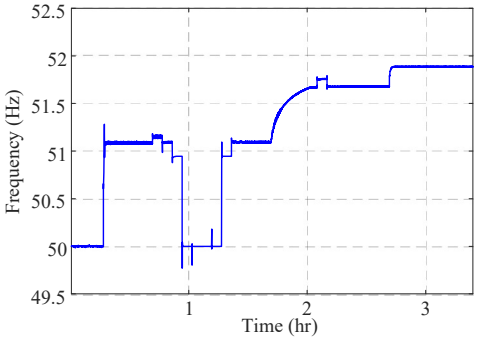

(b)

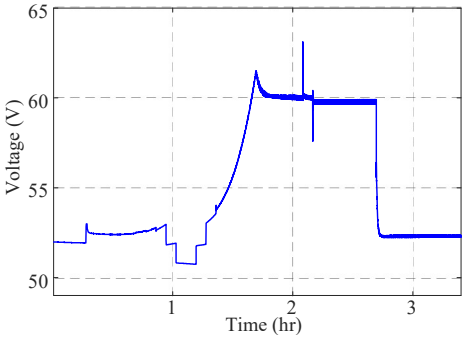

(c)

Fig. 7: Islanded microgrid operation data (a) output power of each unit (b) system frequency (c) battery terminal voltage

$GenSOC_{lb}$, the generator is started up and resynchronized to the microgrid. As described in Section III, the battery is charged at a power level such that the generator runs at 90% loading level in Mode 2. At t = 1.69h (6100s), the generator is tripped and shuts down when battery SOC hits the upper bound $GenSOC_{ub}$. The microgrid operation mode then goes back to Mode 1.

V. Conclusion

The microgrid power flow control presented in this paper not only considers battery power and SOC limits, but also integrates a three-stage charging mechanism, which is more realistic in real-world applications. The three-stage charging mechanism limits battery charging power based on maximum charging power and battery terminal voltage, and allows the battery to be discharged to compensate for load increase with variable PV generation. Two case studies are presented to demonstrate the performance of the proposed control. The

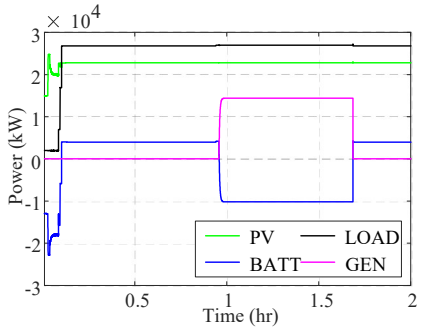

Fig. 8: Mode transition in the islanded microgrid

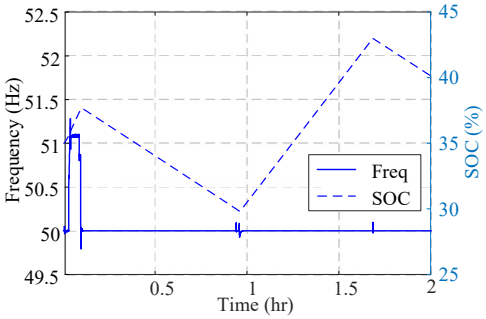

Fig. 9: Frequency of the islanded microgrid and battery SOC

results show that the proposed control is effective in managing battery operating constraints while maintaining the stability of islanded microgrid under different operating conditions.

References

[1] J. Sachs and O. Sawodny, "A two-stage model predictive control strategy for economic diesel-pv-battery island microgrid operation in rural areas," *IEEE Transactions on Sustainable Energy*, vol. 7, no. 3, pp. 903–913, 2016.

[2] B. Belvedere, M. Bianchi, A. Borghetti, C. A. Nucci, M. Paolone, and A. Peretto, "A microcontroller-based power management system for standalone microgrids with hybrid power supply," *IEEE Transactions on Sustainable Energy*, vol. 3, no. 3, pp. 422–431, 2012.

[3] S. Adhikari and F. Li, "Coordinated vf and pq control of solar photovoltaic generators with mppt and battery storage in microgrids," *IEEE Transactions on Smart Grid*, vol. 5, no. 3, pp. 1270–1281, 2014.

[4] C. Sun, G. Joos, and F. Bouffard, "Adaptive coordination for power and soc limiting control of energy storage in islanded ac microgrid with impact load," *IEEE Transactions on Power Delivery*, 2019.

[5] R. Al Badwawi, W. R. Issa, T. K. Mallick, and M. Abusara, "Supervisory control for power management of an islanded ac microgrid using a frequency signalling-based fuzzy logic controller," *IEEE Transactions on Sustainable Energy*, vol. 10, no. 1, pp. 94–104, 2018.

[6] Y. Karimi, H. Oraee, M. S. Golsorkhi, and J. M. Guerrero, "Decentralized method for load sharing and power management in a pv/battery hybrid source islanded microgrid," *IEEE Transactions on Power Electronics*, vol. 32, no. 5, pp. 3525–3535, 2016.

[7] H. Mahmood and J. Jiang, "Autonomous coordination of multiple pv/battery hybrid units in islanded microgrids," *IEEE Transactions on Smart Grid*, vol. 9, no. 6, pp. 6359–6368, 2017.

[8] H. Mahmood and J. Jiang, "Decentralized power management of multiple pv, battery, and droop units in an islanded microgrid," *IEEE Transactions on Smart Grid*, vol. 10, no. 2, pp. 1898–1906, 2017.

[9] J. M. Guerrero, J. C. Vasquez, J. Matas, L. G. De Vicuña, and M. Castilla, "Hierarchical control of droop-controlled ac and dc microgrids - a general approach toward standardization," *IEEE Transactions on Industrial Electronics*, vol. 58, no. 1, pp. 158–172, 2010.

[10] J. Rocabert, A. Luna, F. Blaabjerg, and P. Rodriguez, "Control of power converters in ac microgrids," *IEEE Transactions on Power Electronics*, vol. 27, no. 11, pp. 4734–4749, 2012.